China Steel Technical Report, No. 25, pp. 60－65, (2012)

An Investigation into Hot Deformation Resistance of an AA5083 Alloy

SHI-RONG CHEN*, YHU-JEN HWU, YI-LIANG OU** and YEN-LIANG YEH****

**New Materials Research & Development Department*
***Iron and Steel Research & Development Department*
China Steel Corporation

Quantitative assessments were made over the effects of temperature, work hardening behavior and strain rate sensitivity for an AA5083 alloy using true stress-strain data derived from the friction-free tensile test. Formulae in the forms of a hyperbolic sine equation as well as a combined effect of temperature, strain and strain rate have been constructed for the alloy. The experimental data were well explained by the hyperbolic sine equation using the measured activation energy for hot deformation. It was found that peak strain plays a decisive role on the accuracy of a numerical approach to the work hardening behavior. Through the application of the present formulae, deviations between the calculated and the measured rolling force during hot rolling were largely suppressed and the mass productions of AA5083 alloy plates with superior dimensional precision in the hot rolling mill at CS aluminum have been successfully achieved.

Keywords: Deformation resistance, Work hardening, Strain rate sensitivity, Activation energy, Homologous temperature

1. INTRODUCTION

AA5083 alloy plates are widely applied to the transportation, electronics and solar energy industries. Superiorly precise dimensional quality of the hot-rolled plates is specified for the construction of vacuum chambers. It is well known that gauge variation of the plates strongly depends on an accurate control of roll gap, which is a function of mill modulus and separating force. This force, in turn, is correlated with mean flow stress, deformation resistance of the material, rolling speed and geometrical parameters of the roll gap by a force model, as predicted by Sims formula[1]. Thus, a prediction formula for the deformation resistance of an alloy plays a decisive role in the minimization of the thickness deviations during hot rolling.

Two categories of models have already been proposed so far. Firstly, dependence of steady-state stress σ is described by a hyperbolic sine equation[2-5], originating from earlier creep studies. This equation has been proven to be able to accurately extend over several orders of magnitude differences of both the flow stress and the strain rate[3]. Its mill application, however, is limited because rolling strain ε is excluded. On the other hand, many commercialized equations have been constructed by Japanese workers[6-9] using an additive link through the effects of temperature, strain and strain rate, as will be discussed later.

Formulae currently available for the deformation resistance of AA5××× alloys as well as their basic forms are listed in Table 1, where Equations 2, and 5-7 are valid for 5083, and Equation 4 for 5052 alloy. Evidently, the formulation differs entirely from one to another. In the basic form of the hyperbolic sine equation, Z is the Zener-Hollomon parameter[10], Q is the activation energy for hot deformation, R is the universal gas constant, T is the test temperature in Kelvin scale, and A, α and n are material constants, respectively. All the equation constants in Table 1 have been normalized for the stress to be expressed in the unit of MPa. For instance, the Q in Sheppard's equation is 171400 J/mol.

Equations 4-7 follow the basic form of Equation 3 and Shida's work for steels [11], where n is the work hardening exponent, and m is the strain rate sensitivity factor of the material. Equation 4 is similar to Equation 5 on the analysis of temperature effect, nevertheless homologous temperature Th, test temperature normalized by solidus, was used in Chida's equation, whereas Kelvin temperature in Motomura's. Moreover, n and m are temperature dependent in Equation 5, while constant values were respectively adopted in Equations 4 and 6. Equation 6 has a similar $f(\varepsilon^n)$ term to that in Equation 5, but the temperature and the stress are approached in a different way where α_k is a constant

Table 1 Prediction formulae for the hot deformation resistance of AA5××× alloys

Author	Prediction formula
	Basic equation: $Z = \dot{\varepsilon} \times e^{Q/RT} = A \times [\sinh(\alpha\sigma)]^n$ ····· (1)
Sheppard	$\mathrm{Ln}(Z = \dot{\varepsilon} \times e^{171400/RT}) = 23.11 + 4.99\ \mathrm{Ln}[\sinh(0.015 \times \sigma)]$ ····· (2)
	Basic equation: $\sigma = f(T) \times f(\varepsilon^n) \times f(\dot{\varepsilon}^m)$ ····· (3)
Motomura	$\sigma = (196.7 - 321.2/T + 169.7/T^2) \times \varepsilon^{0.079} \times \dot{\varepsilon}^{0.112}$ ····· (4)
Chida	$\sigma = (101.44 - 251.6/Th + 218.7/Th^2) \times [1.06 \times (\varepsilon/0.2)^{-0.257Th + 0.237} - 0.06 \times (\varepsilon/0.2)] \times (\dot{\varepsilon}/7)^{0.274Th - 0.151}$ ··· (5)
Kitamura	$\sigma = 31.4 \times \alpha_k \times \sigma_{0.2} \times \mathrm{Ln}(1000/T) \times [1.14 \times (\varepsilon/0.2)^{0.23} - 0.14 \times (\varepsilon/0.2)] \times (\dot{\varepsilon}/10)^0$ ····· (6)
Takuda	$\sigma = [(2.3 + 1.61\Sigma C_1) \times \mathrm{Ln}(\dot{\varepsilon} \times e^{142000/RT}/10^{12}) + (26.0 + 14.6\Sigma C_1)] \times (\varepsilon/0.2)^n$ ····· (7)
	$0 < \varepsilon \le 0.2$: $n = (-32.5\ \Sigma C_2 + 285) \times (1/T - 1/573) - 0.048\ \Sigma C_2 + 0.25$ ····· (7a)
	$0.2 < \varepsilon \le 0.7$: $n = (-44.3\ \Sigma C_2 + 380) \times (1/T - 1/573) - 0.0683\ \Sigma C_2 + 0.25$ ····· (7b)
	ΣC_1 = total alloy concentrations + 0.7× Mg (wt%) ····· (7c)
	ΣC_2 = total alloy concentrations - 0.3× Mg (wt%) ····· (7c)

and $\sigma_{0.2}$ is the material strength at a strain of 0.2 under room temperature. The uniqueness of Equation 7 is that alloy compositions ΣC and effect of Mg were introduced, while the $f(\dot{\varepsilon}^m)$ term was excluded and the activation energy for self-diffusion, 142,000 J/mol, was applied for all aluminum alloys.

Hot deformation resistance of aluminum alloys is widely assessed using a plain strain compression or a cam plastometer. True stress-strain curves are obtained after a correction for the friction hill, where coefficient of friction is usually measured by the ring test proposed by Male[12]. Although resultant stress level is strongly influenced by the correction, detailed information about the coefficient of friction has been limited so far.

Since data scatterings of the ring test were encountered, a tensile test was chosen in the present work because it is a friction-free process, in which homogeneous deformation is sustained far beyond the maximum stress level until the commencement of necking, as reported by Voce[13]. Limited elongation could be one drawback of the test, but this is considered to be negligible for the AA5083 plates because the pass reductions during finish rolling stage are relatively light.

Detailed understandings of the published formulae, particularly Equations 5 and 7, are considered to be indispensable for the modernizing the hot rolling mill at CS Aluminium. Thus, quantitative analysis over the effects of temperature, strain rate sensitivity and work hardening behavior on the hot deformation resistance of an AA5083 alloy was carried out in this paper. It was hoped that appropriate formulae could be derived for the mass production of the alloy plates with superior dimensional quality.

2. EXPERIMENTAL PROCEDURES

Samples were cut from a direct chill cast slab having a dimension of 520 mm thick and 1660 mm wide. The major chemical compositions of the alloy are listed in Table 2. Prior to the sampling, the slab was homogenized to a peak temperature of 520°C and soaked there for 8 hours in the cast house of CS Aluminium. Characterization of the constituent phases and microstructural details for this alloy have been published elsewhere[14], where two types of intermetallic compounds were observed: the Fe-enriched, consisting of $Al_6(Fe,Mn)$, Al_3Fe, α–AlFeSi; and the Mg-enriched compounds. The latter compounds were identified mostly as Mg_2Si by electron microscopy after the Mg-enriched particles were slice-cut using a focused ion beam.

The samples were subsequently machined into

Table 2 The major alloying compositions of the AA5083 alloy (wt%)

Si	Fe	Cu	Mn	Mg	Cr	Ti	Al
0.11	0.28	0.03	0.69	4.54	0.08	0.014	balance

round specimen, with diameter of 6.25 mm and gauge length of 25 mm, according to ASTA A370. Tensile elongation was found to decrease with increasing depth from the free surface of the slab presumably due to variations of the cast structure and internal porosities as reported by Nagaumi[15]. To minimize the deviations, the specimen was carefully sectioned in the following way: longitudinal axis was kept vertical to the rolling plane and mid-point of the gauge length was located at a constant depth of 70 mm below the free surface. Tensile tests were carried out with an MTS 810 machine coupling with an electric heating furnace, measurements were undertaken after the preset target temperature stabilized and the specimen soaked for another 30 minutes.

3. RESULTS AND DISCUSSION

3.1 Stress- strain curves

It was found that the flow stress and work hardening behavior of the alloy changed greatly with variations of the temperature, strain and strain rate. Figure 1 shows temperature dependence of the stress-strain curves at 225-475°C under a nominal strain rate of 0.55 s^{-1}. As expected, flow stress increased with decreasing the temperature, whereas elongation decreased. It can be seen that at the low temperatures, for example at 225°C, the curve is dominated by work hardening so that the stress increases progressively with increasing the strain. Degree of work hardening, however, decreases gradually with increasing the temperature and then work softening appears at the higher temperatures. As a result, at 475°C, the stress increased rapidly to a peak state and then dropped gradually, that is to say work softening occurred, at the higher strains. At the intermediate temperatures, for example 325-375°C, both work hardening and work softening were observed: the alloy work hardened initially, but the degree of the work hardening decreased with increasing the strain, and work softening subsequently appeared beyond the peak stress and persisted until the occurrence of necking before the final fracture.

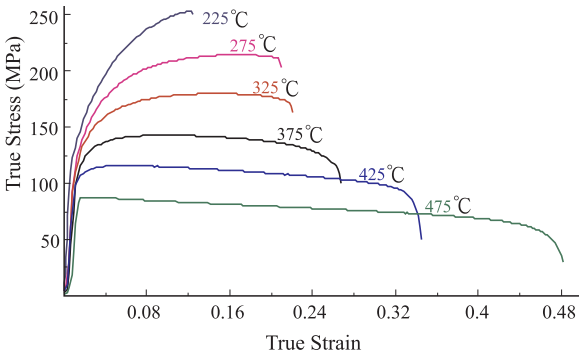

Fig.1. Temperature dependence of the stress-strain curves under a nominal strain rate of 0.55 s^{-1}.

Strain rate dependence of the flow curves tested at 450°C is given in Fig.2. It is evident that the stress level and degree of work hardening increase with an increasing the strain rate, while the elongation decreases.

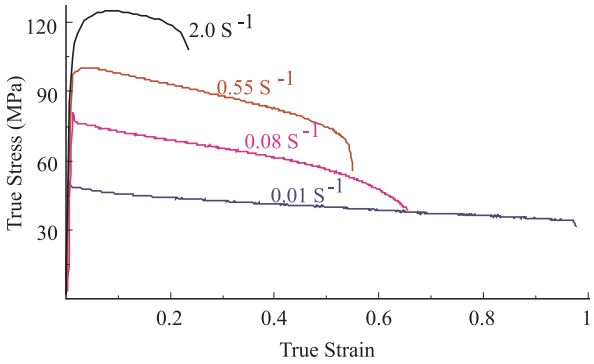

Fig.2. Strain rate dependence of the flow curves tested at 450°C.

3.2 Hyperbolic Sine Equation

The stress at a strain of 0.15 for each curve was obtained for the derivation of Q, the activation energy for hot deformation, as reported previously[3]. For this, strain rate dependence against stress, using a value for α of 0.05 MPa^{-1}, is given in Fig.3a, the stress against temperature in Fig.3b. The slope of each curve was obtained via a linear regression analysis, respectively, and then averaged. Through a simple multiplication over the two mean slopes and the universal gas constant R, the experimental Q was determined to be 173200 J/mol, close to that reported by Sheppard [4].

The measured Q was subsequently used to calculate Z, the Zener-Hollomon parameter, and analyzed according to Equation 1[3-5] for a quick estimate of the flow stress during hot deformation. As a result, the following equation was drawn.

$$\text{Ln } Z = 20.58 + 1.73\ [\text{Ln sinh}(\alpha\sigma)] \quad \cdots\cdots\cdots\cdots \quad (8)$$

A comparison of the data scatterings of Equation 8 and Sheppard's Equation 2 is demonstrated in Fig.4, where the black bold line is calculated by Eq. 8 and the grey line, by Eq. 2. It is clear that the measured data are very well explained by Eq. 8, supporting the point of view that the flow behavior at elevated temperatures under high strain rate conditions is a thermally activated process, thus the stress can be satisfactorily predicted using the earlier creep equation[2-3]. The deviations in Equation 2 are mostly appear at both the high and the low Z regions, presumably due to differences in alloying compositions because the equation constant of the hyperbolic sine term increases with an increasing purity of the material.

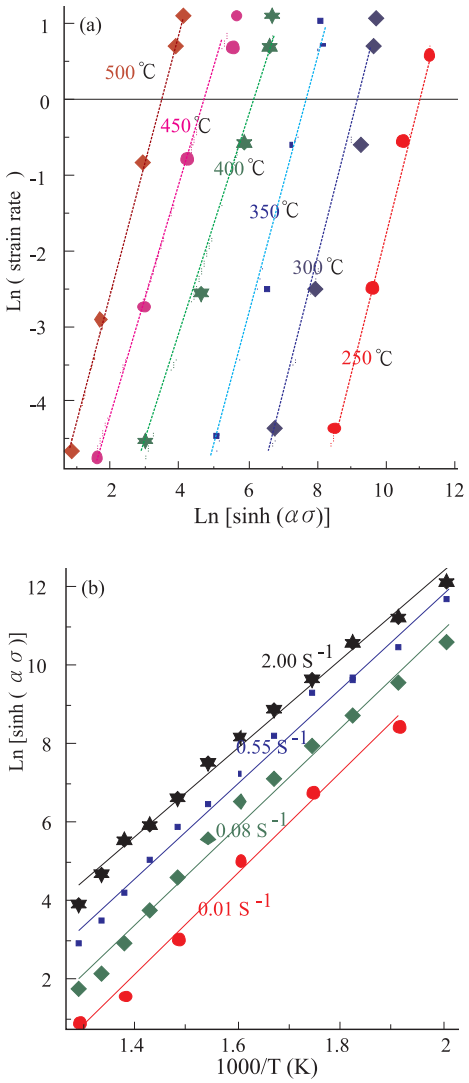

Fig.3. Activation energy for hot deformation Q is derived from the curves of (3a) dependence of strain rate against stress, (3b) dependence of stress against temperature.

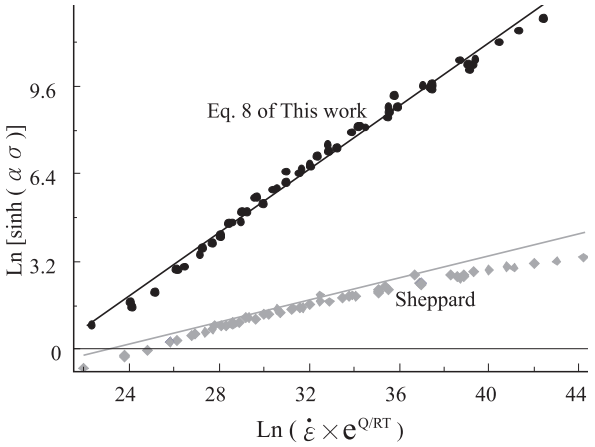

Fig.4. The measured data are very well explained by Eq. 8.

3.3 Effects of strain rate, temperature and work hardening behaviors

Another approach following the basic Equation 3 was subsequently carried out to describe the combined effect of the strain rate sensitivity, temperature and work hardening behaviors[6-9] for mill applications. The strain rate sensitivity factor (m) was found to increase progressively with increasing temperature, as shown in Fig.5, which is consistent with Lloyd's observation[16], but contrary to the formulation of Motomura et al.[7-9] that m was a constant. Calculated m values using Chida's Equation 5[6] are also plotted in Fig.5. It can be seen that underestimation occurs from applying Chida's equation but the reason is not clear. Further analysis suggested that m could be described by using a standard strain rate of 2 s^{-1} and solidus 843K for the calculation of homologous temperature (Th)[6], and the following equation was drawn:

$$f(\dot{\varepsilon}^{m}) = (\dot{\varepsilon}/2)^{0.37Th-0.19} \quad \cdots\cdots\cdots\cdots\cdots\cdots\cdots\cdots \quad (9)$$

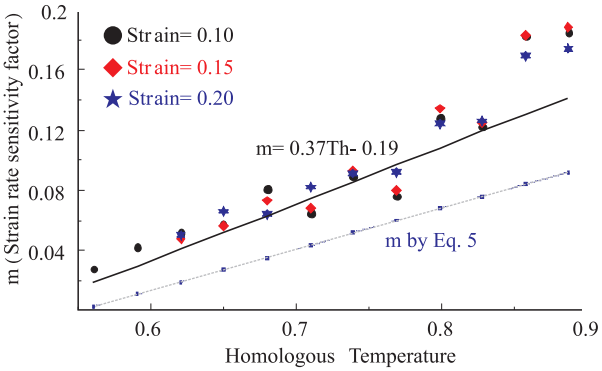

Fig.5. Strain rate sensitivity factor m increases with increasing temperature.

A binomial function[6,7] was subsequently applied for the temperature effect, using Th, although the flow stresses have been observed to vary in a roughly linear way against temperature in Fig.3b. Prior to this, the measured stresses were normalized according to Eq. 9. Figure 6 shows that the normalized stresses at strains of 0.10-0.25 and strain rates of 0.08-2.0 s^{-1} correspond well with the bold line, which is described by the following parabolic function, Eq. 10. The stresses under other test conditions displayed similarly in spite of minor changes for the equation constants.

$$f(T) = -570 + 814/Th - 195/Th^{2} \quad \cdots\cdots\cdots\cdots \quad (10)$$

The work hardening exponent (n) was confirmed to increase with decreasing temperature as well as increasing the strain rate generally. Nevertheless, a close examination over the curves, such as those shown in Fig.1, revealed that n was a positive constant at the low

temperatures, it decreased gradually and then turned to negative with increasing the strain at the intermediate temperatures of 325-375°C, and it turned to negative at the high temperatures. Thus, a precise description for such phenomena is intrinsically difficult.

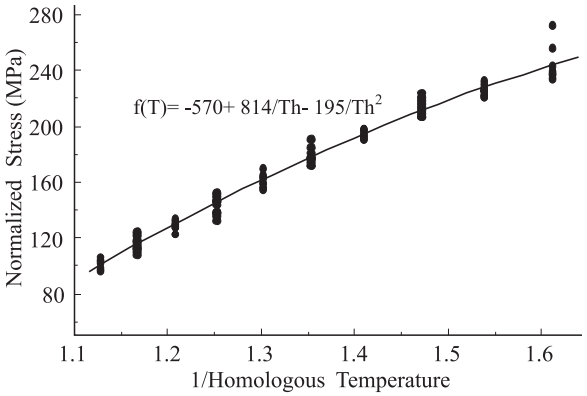

Fig.6. The measured stresses normalized by f ($\dot{\varepsilon}^{m}$) correspond with calculations by Eq. 10.

As reported by Shida[11], deviations of f(ε^{n}) could be minimized through a careful choice of the reference strain, with 0.20 having been satisfactorily proven for steels and widely applied to aluminum alloys[6,8,9]. However, large variations were encountered using the strain 0.2 for the presently measured data. It was found that the variations were minimized when a peak strain of 0.14 was introduced so that the shape of the stress-strain curves could be satisfactorily described. As a result, the work hardening term is described by following equation:

$$f(\varepsilon^{n}) = 1.16\times (\varepsilon/\varepsilon_{p})^{-0.45Th+0.42} - 0.13\times (\varepsilon/\varepsilon_{p}) \cdots\cdots (11)$$

Figure 7 shows that the simulated stress-strain curves using Eq. 11 are close to the measured data although deviations appeared at the strains lower than 0.05.

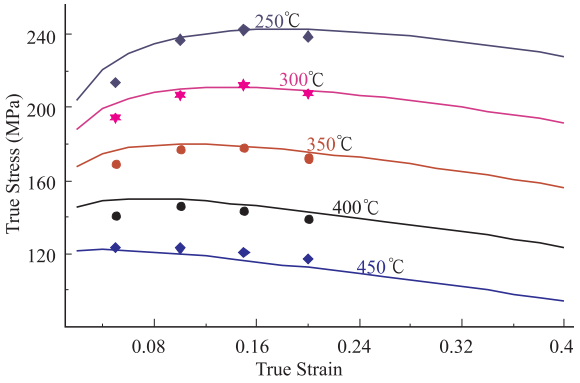

Fig.7. Comparison of the simulated stress-strain curves using Equation 11 and the measured data under a nominal strain rate of $2s^{-1}$.

With an additive combination of Equations 9 to 11, a new formula Equation 12 was consequently derived for predicting hot deformation resistance of the AA5083 alloy, under the temperatures of 250-475°C, strains of < 0.40 and strain rates of 0.08-2.0s^{-1} :

$$\sigma = f(T)\times f(\varepsilon^{n})\times f(\dot{\varepsilon}^{m}) = (-570 + 814/Th - 195/Th^{2})\times$$
$$[1.16\times(\varepsilon/\varepsilon_{p})^{-0.45Th+0.42} - 0.13\times(\varepsilon/\varepsilon_{p})]\times(\dot{\varepsilon}/2)^{0.37Th-0.19} \cdots\cdots (12)$$

Figure 8 shows a comparison for the present equation and the previously proposed equations. It can be seen that the measured data are well explained by the present formula, whereas an underestimate occurs in Takuda's equation (Eq. 7) and relatively large variations appears in that of Equation 5 particularly at the higher stresses.

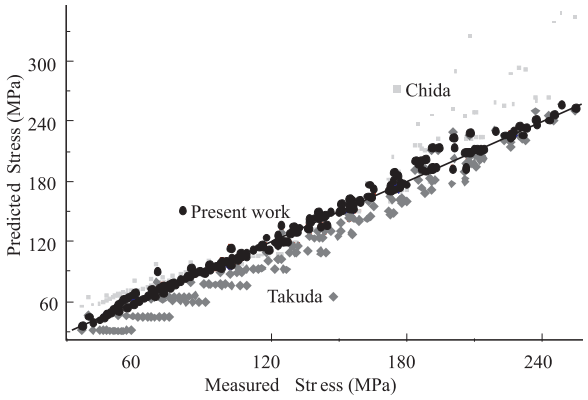

Fig.8. Comparison of Equation 12 and those proposed by Chida and Takuda using the measured data.

3.4 Application of the present work

The present work was then applied to the rolling mill at CS Aluminium through formula modifications for the hot deformation resistance and links were appropriately made to the force model. Discrepancies between the predicted and the measured forces were effectively suppressed resulting in a significant improvement in the gauge variations. As a result, the development of hot-rolled AA5083 alloy plates with superior dimensional quality has been successfully achieved.

4. CONCLUSIONS

The hot deformation behaviors of the AA5083 alloy under uni-axial tension have been thoroughly examined for the mass production of hot-rolled plates with a superiorly precise dimensional quality. Through

quantitative assessments over the effects of the temperature T, strain ε and strain rate $\dot{\varepsilon}$, following conclusions are drawn:

1. By using an α value of 0.05 MPa^{-1} and 173200 J/mol, the experimental activation energy for hot deformation, the flow stress σ can be described by the equation of:

$$\mathrm{Ln}\,(\dot{\varepsilon} \times e^{Q/RT}) = 20.58 + 1.73 \times \mathrm{Ln}[\sinh(\alpha\sigma)]$$

2. When strain term is involved, the flow stress can also be described by the equation of:

$$\sigma = (-570+814/Th-195/Th^2) \times [1.16 \times (\varepsilon/\varepsilon_p)^{-0.45Th+0.42}-0.13\times(\varepsilon/\varepsilon_p)] \times (\dot{\varepsilon}/2)^{0.37Th-0.19}$$

The equation has been derived from the test conditions of 250-475°C, strains <0.40, and strain rates 0.08-2.0s^{-1}, and uses the experimental peak strain 0.14 as well as homologous temperature Th.

REFERENCES

1. R.B. Sims：Proc. Inst. Mech. Eng., ”The Calculation of Roll Force and Torque in Hot Rolling Mills”, 1954, 168, pp. 191-200.
2. C.M. Sellars and W.J. McG. Tegart：Intern. Metall. Rev., ”Hot Workability”, 1972, vol. 17, pp. 1-24.
3. W.A. Wong and J.J. Jonas: Trans. The Metall. Soc. AIME, "Aluminum Extrusion as a Thermally Activated Process", 1968, vol. 242, pp. 2271-2280.
4. T. Sheppard: Proceedings 8th Light Metal Congress, "Extrusion Processing of Aluminum Alloys", 1987, pp. 301-311.
5. H. Yoshida and H. Tanaka: Sumitomo Light Metal Technical Reports, “High Temperature Deformation of Aluminum Alloys”, 2008, vol. 49, 1, pp.87-106.
6. N. Chida, H. Kimura and Y. Baba: Sumitomo Light Metal Technical Reports, ”Study on the Flow Stress of Aluminum and Aluminum Alloys at High Temperature”, 1978, vol. 19, no. 1-2, pp. 3-11.
7. M. Motomura, S. Shimamura and T. Nishimura: J. Japan Institute of Light Metals, ”On Relating the Resistance to Deformation of Commercial Pure Aluminum and Aluminum Alloy”, 1976, vol. 26, no. 9, pp. 432-440.
8. H. Takuda, S. Kikuchi and N. Hatta: J. Japan Society for Technology of Plasticity, ”Modeling of Comprehensive Formula for Flow Curves of Aluminum Alloys at Elevated Temperatures”, 1993, vol. 34, no.385, pp.165-170.
9. S. Kitamura and S. Tamiya: Kobe Steel Engineering Reports, ”Computerization of Hot Rolling for Aluminum Alloys”, 1978, vol. 28, no. 2, pp. 94-96.
10. Zener and J.H.Hollomon：J. Applied Physics, “Effect of strain rate upon plastic flow of steel”, 1944, vol. 15, pp. 22-32.
11. S. Shida: Hitachihyolon (in Japanese), “Resistance of Metals to Compression and Rolling Loads”, 1965, vol. 47, no. 9, pp. 57-62.
12. A.T. Male and M.G. Cockcroft: J. Inst. Met., “A method for determination of the coefficient of friction of metals under conditions of bulk plastic deformation”, 1964-5, vol. 93, pp. 38-46.
13. E. Voce: J. Inst. Metals, “The relationship between stress and strain for homogeneous deformation”, 1948, vol. 74, pp. 537-562.
14. Shi-Rong Chen, Kuo-Feng Hsu: China Steel Technical Report, “Microstructural Evolution of AA 5083 Re-Rolled Aluminum Casts during Homogenizing Process”, 1999, 13, pp. 38-48.
15. H. Nagaumi, K. Komatsu, N. Hagigawa and Y. Nishikawa: J. Japan Institute of Light Metals, “Observation of Porosity Distribution in Al-4.4Mg DC Slab and Porosity Formation”, 1998, vol. 48, no. 6, pp. 265-275.
16. D.J. Lloyd: Metall. Trans., "The Deformation of Commercial Aluminum-Magnesium Alloys", 1980, 11A, pp. 1287-1294. □